The Nonlinear Schrödinger Equation As a Model Of Superfluidity

Paul H. Roberts and Natalia G. Berloff

Department of Mathematics
University of California, Los Angeles, CA, 90095-1555
roberts@math.ucla.edu, nberloff@math.ucla.edu

Abstract. The results of theoretical and numerical studies of the Gross-Pitaevskii (GP) model are reviewed. This model is used to elucidate different aspects of superfluid behaviour: the motion, interactions, annihilations, nucleation and reconnections of vortex lines, vortex rings, and vortex loops; the motion of impurities; flow through apertures; superfluid turbulence and the capture of impurities by vortex lines. The review also considers some generalizations of the model.

1 Introduction

One of the most useful ways of describing superfluid helium at zero temperature begins with Schrödinger's equation for the one-particle wave function Ψ. Since liquid helium is a strongly correlated system dominated by collective effects, the form of the Hamiltonian in Schrödinger's equation cannot be derived starting from first principles. At zero temperature ^{4}He has large interatomic spacing and low density, which suggests a description in terms of a weakly interacting Bose gas for which such a derivation can be made rigorous. Continuum mechanical equations for ^{4}He are usually built on the assumption that a Bose condensate gives the exact description at zero temperature.

The imperfect Bose condensate in the Hartree approximation is governed by equations that were derived by Ginsburg and Pitaevskii [22] and by Gross [26], and generally called "GP equations". In terms of the single-particle wavefunction $\Psi(\mathbf{x},t)$ for N bosons of mass M, the time-dependent self-consistent field equation is

$$\mathrm{i}\hbar\Psi_t = -\frac{\hbar^2}{2M}\nabla^2\Psi + \Psi\int |\Psi(\mathbf{x}',t)|^2 V(|\mathbf{x}-\mathbf{x}'|)\, d\mathbf{x}', \tag{1}$$

where $V(|\mathbf{x}-\mathbf{x}'|)$ is the potential of the two-body interactions between bosons. The normalization condition is

$$\int |\Psi|^2\, d\mathbf{x} = N. \tag{2}$$

For a weakly interacting Bose system, (1) is simplified by replacing $V(|\mathbf{x}-\mathbf{x}'|)$ with a δ - function repulsive potential of strength V_0. This does not alter the nature of the results since the characteristic length of the weakly interacting Bose gas is larger than the range of the force [26]. Equation (1) for such a potential is

$$\mathrm{i}\hbar\Psi_t = -\frac{\hbar^2}{2M}\nabla^2\Psi + V_0|\Psi|^2\Psi. \tag{3}$$

Equations (1)-(3) define Hamiltonian systems, the following integrals being conserved: mass

$$\mathcal{M} = M \int |\Psi|^2 \, d\mathbf{x}, \tag{4}$$

momentum density

$$\mathbf{p} = \frac{\hbar}{2\mathrm{i}} \int [\Psi^* \nabla \Psi - \Psi \nabla \Psi^*] \, d\mathbf{x}, \tag{5}$$

and energy; in the case of (3) this is expressed by

$$\mathcal{E} = \frac{\hbar^2}{2M} \int |\nabla \Psi|^2 \, d\mathbf{x} + \frac{V_0}{2} \int |\Psi|^4 \, d\mathbf{x}. \tag{6}$$

Our starting point is a condensate everywhere at rest in what we shall call the “laboratory frame”, so that $\Psi = \exp(\mathrm{i}E_v/\hbar)$ in that frame, where E_v is the chemical potential of a boson (i.e., the increase in ground state energy when one boson is added to the system). We then consider deviations from that state by studying the evolution of ψ where

$$\psi = \Psi \exp(\mathrm{i}E_v t/\hbar), \tag{7}$$

so that (3) becomes

$$\mathrm{i}\hbar\psi_t = -\frac{\hbar^2}{2M}\nabla^2\psi + V_0|\psi|^2\psi - E_v\psi. \tag{8}$$

It is usually convenient to model phenomena in an infinite domain in which, prior to the onset of a disturbance, $\psi = \psi_\infty$ everywhere, where, by (8)

$$\psi_\infty = (E_v/V_0)^{1/2}. \tag{9}$$

We then modify (4)-(6) to forms measuring departures from this uniform state (see, e.g. [44])

$$\int (|\psi|^2 - \psi_\infty^2) \, d\mathbf{x} = 0, \tag{10}$$

$$\mathbf{p} = \frac{\hbar}{2\mathrm{i}} \int [(\psi^* - \psi_\infty)\nabla\psi - (\psi - \psi_\infty)\nabla\psi^*] \, d\mathbf{x}, \tag{11}$$

$$\mathcal{E} = \frac{\hbar^2}{2M} \int |\nabla\psi|^2 \, d\mathbf{x} + \frac{V_0}{2} \int (|\psi|^2 - \psi_\infty^2)^2 \, d\mathbf{x}. \tag{12}$$

The mass density and flux are

$$\rho = M\psi\psi^*, \qquad \mathbf{j} = \frac{\hbar}{2\mathrm{i}}((\psi^* - \psi_\infty)\nabla\psi - (\psi - \psi_\infty)\nabla\psi^*). \tag{13}$$

2 The fluid equations

One of the principal aims of this review is to interpret the consequences of the condensate model, not from the perspective of solid state physics, but through the eyes of a fluid dynamicist. This is achieved by recasting the nonlinear Schrödinger equation by the Madelung transformation. We write

$$\psi = R\mathrm{e}^{\mathrm{i}S}, \tag{14}$$

so that

$$\rho = MR^2, \qquad \mathbf{j} = \rho\mathbf{u} = \rho\nabla\phi, \qquad \phi = (\hbar/M)S. \tag{15}$$

The real and imaginary parts of (8) then yield a continuity equation

$$\frac{\partial\rho}{\partial t} + \nabla\cdot(\rho\mathbf{u}) = 0, \tag{16}$$

and an integrated form of the momentum equation

$$\frac{\partial\phi}{\partial t} + \frac{1}{2}u^2 + c^2\left(\frac{\rho}{\rho_\infty} - 1\right) - c^2a^2\frac{\nabla^2\rho^{1/2}}{\rho^{1/2}} = 0, \tag{17}$$

where ρ_∞ is the density at infinity and c is the speed of sound:

$$\rho_\infty = M\psi_\infty^2, \qquad c^2 = E_v/M = (V_0/M^2)\rho_\infty. \tag{18}$$

The last term in (17) is sometimes called the "quantum pressure" although it is dimensionally a chemical potential. It is significant where "healing" of the wavefunction ψ is important, as for instance in a vortex core, or within a "healing layer" adjacent to a boundary, of approximate thickness

$$a = \frac{\hbar}{(2ME_v)^{1/2}}, \tag{19}$$

which is called the "healing length". Elsewhere, in the "bulk" of the fluid, the last term in (17) in insignificant, and (17) assumes the form appropriate for a classical inviscid fluid, in which the pressure, P, is proportional to ρ^2.

The unintegrated form of the momentum equation is obtained by taking the gradient of (17). This gives

$$\rho\left(\frac{\partial u_i}{\partial t} + u_j\frac{\partial u_i}{\partial x_j}\right) = -\frac{\partial P}{\partial x_i} + \frac{\partial\Sigma_{ij}}{\partial x_j}, \tag{20}$$

where P is pressure and the Σ_{ij} are the quantum stresses

$$P = \frac{V_0}{2M^2}\rho^2, \quad \Sigma_{ij} = \left(\frac{\hbar}{2M}\right)^2\rho\frac{\partial^2\ln\rho}{\partial x_i\partial x_j}; \tag{21}$$

see [24].

Curves on which the wavefunction ψ vanishes correspond to vortex lines in the superfluid with the correct unit of quantization, $\kappa = h/M$. For simple zeros, of the kind with which we shall be concerned, the circulation

$$C = \int_{\Gamma} \mathbf{u} \cdot \, d\mathbf{s} \tag{22}$$

round a closed contour Γ is equal to the number of vortex lines that Γ contains. Since $\mathbf{u} = \rho \nabla \phi$, the circulation C is preserved until a vortex line crosses Γ, whereupon C increases or decreases by κ. At the instant at which the vortex line meets Γ, the density ρ on Γ is zero at the point of intersection; Γ is no longer a closed curve, and Kelvin's theorem on the constancy of C is inapplicable.

This marks an extremely basic difference between the condensate equations and the Euler equations of classical fluid dynamics. Both describe conservative (Hamiltonian) systems, but the Euler fluid does not allow circulation to change. In describing topological changes in the vorticity of a classical fluid, it is necessary to invoke a mechanism that breaks the constraint of Kelvin's theorem. For example, one method of modeling the severing or coalescence of vortex filaments is to restore viscosity to the fluid, so allowing the vorticity to diffuse from one filament to the other. Another method is described in §5 below. Such devices are unnecessary when the condensate model is employed.

The GP model not only enjoys the advantage of comparative simplicity but also describes qualitatively correct superfluid behaviors at low temperatures T. In this paper we review how the GP model is successfully used to elucidate the motion, interactions, annihilations, nucleation and reconnections of vortex lines, vortex rings, and vortex loops; the motion of impurities; the flow of superfluid through apertures; superfluid turbulence; and the capture of impurities by vortex lines.

3 Shortcomings of the GP model

Despite its success, several aspects of the local model (8) are qualitatively or quantitatively unrealistic for superfluid helium. The dispersion relation between the frequency, ω, and wave number, k, of sound waves according to (8) is

$$\omega^2 = c^2 k^2 + \left(\frac{\hbar}{2M}\right)^2 k^4. \tag{23}$$

The velocity, c, of long wavelength sound waves is therefore proportional to $\rho^{\frac{1}{2}}$ see (21). (We have here denoted the bulk density, ρ_∞, by ρ.) That this is unrealistic is seen from the experiments on Grüneisen constant $U_G = (\rho \partial c / c \partial \rho)_T$, which shows that, in the bulk (i.e., on length scales long compared with the healing length, κ/c), the fluid behaves as a barotropic fluid ($p \propto \rho^\gamma$) with $\gamma = 2.8$ (see [10] and references therein).

By writing $p = \hbar k$ and $\epsilon(p) = \hbar\omega$, we convert (23) into the dispersion curve of GP theory:

$$\epsilon(p) = p \left[c^2 + (p/2M)^2\right]^{1/2}. \tag{24}$$

At best, this describes the phonon branch of the excitation spectrum. The roton branch is lost. At first sight this does not seem important, because it is only the phonon branch that is thermally populated at low temperatures. Nevertheless, the lack of a roton branch is seen to be serious when, as in §§6 and 7 below, we use the GP model to simulate superflow past boundaries. We shall describe in §8 a generalization of (8) that restores the roton branch.

To expose a related deficiency of the GP model, we invoke the "ghost" of a normal fluid by supposing that T is infinitesimal but nonzero. In local thermodynamic equilibrium, the density of quasi-particles in the fluid is

$$N_q = \frac{1}{\hbar^3}\int \left[\exp\left(\frac{\epsilon - \mathbf{w}\cdot\mathbf{p}}{kT}\right) - 1\right]^{-1} d\mathbf{p}, \tag{25}$$

where $\mathbf{w} = \mathbf{u}_n - \mathbf{u}_s$, is the velocity of the normal fluid[1] relative to the superfluid; e.g. see [34]. It is clear from (24) that N_q is negligibly small when $w < c$, because then $\epsilon - \mathbf{w}\cdot\mathbf{p} > 0$ for all $\mathbf{p}$. When $w > c$, however, the integrand in (25) is negative and even infinite for $\mathbf{p}$ for which $\epsilon - \mathbf{w}\cdot\mathbf{p} \le 0$. This unphysicality shows that the assumption of local thermodynamic equilibrium is untenable wherever $w > c$. Then quasi-particle production destroys superfluidity.

In real superfluid helium, the limiting value of w for the destruction of superflow is known as the 'Landau critical velocity'; we shall denote this by u_L. The argument just given correctly indicates that u_L is determined by a condition of tangency: $u_L = \epsilon(p)/p = d\epsilon(p)/dp$ and, because of the roton branch, this is much less than c for superfluid helium. Compressibility therefore plays a greater role in the condensate than in real helium.

GP theory has no preferred reference frame. This is hardly surprising in a model which applies at $T = 0$, where not even the "ghost" of normal fluid exists. Nevertheless, it is a non-uniformity for $T \to 0$ that is an undesirable attribute of GP theory. Carlson [13] proposed a way of removing this by augmenting (8) with a term motivated by Khalatnikov's (1952) theory of mutual friction between the superfluid and normal fluid at finite T, which involved three independent kinetic coefficients, of which only the third, $\zeta_3 (> 0)$, concerns us here. Khalatnikov modified the integrated superfluid momentum equation to be

$$\frac{\partial\phi}{\partial t} + \frac{1}{2}u_s^2 + \mu = -\zeta_3 \nabla\cdot(\rho_s \mathbf{w}), \tag{26}$$

where μ is a chemical potential; Using the mass conservation equation

$$\frac{\partial\rho}{\partial t} + \nabla\cdot(\rho\mathbf{u}) = 0, \tag{27}$$

[1] We are attempting here to make a point of principle, and for this purpose we may ignore the fact that the mean free path of phonons at low temperatures may be so large that they are better represented by a Boltzmann equation than by a normal fluid continuum. We temporarily write the density of the superfluid and normal fluid by ρ_s and ρ_n (where $\rho_s + \rho_n = \rho$) and their velocities as $\mathbf{u}_s$ and $\mathbf{u}_n$ (where $\rho\mathbf{u} = \rho_s\mathbf{u}_s + \rho_n\mathbf{u}_n$ is the total momentum density).

we see that (26) can also be written as

$$\frac{\partial \phi}{\partial t} + \frac{1}{2}u_s^2 + \mu = -\zeta_3 \nabla \cdot \left(\frac{\partial \rho}{\partial t} + \nabla \cdot (\rho \mathbf{u}_n) \right). \tag{28}$$

Since $\rho \approx \rho_s$ for small T, this suggests that a useful generalization of (8) is

$$\mathrm{i}\hbar\psi_t = -\frac{\hbar^2}{2M}\nabla^2\psi + V_0|\psi|^2\psi - E_v\psi + \zeta M^2\psi\left[\partial_t|\psi|^2 + \nabla\cdot(|\psi|^2\mathbf{u}_n)\right], \tag{29}$$

where $\zeta > 0$. This implies, in place of (17),

$$\frac{\partial \phi}{\partial t} + \frac{1}{2}u^2 + c^2\left(\frac{\rho}{\rho_\infty} - 1\right) - c^2a^2\frac{\nabla^2\rho^{1/2}}{\rho^{1/2}} = -\zeta\left(\frac{\partial \rho}{\partial t} + \nabla\cdot(\rho\mathbf{v}_n)\right), \tag{30}$$

and (16) is unchanged. Unlike (1) or (8) equations (29) and (30) single out a preferred reference frame, the one in which $\mathbf{v}_n = 0$. It is reasonable to suppose that $\zeta \to 0$ as $T \to 0$ since otherwise the normal fluid, which is subjected to the frictional force that is the counterpart of the ζ term in (30), would be infinitely accelerated in the limit.

Let us again suppose infinitesimal but nonzero T, and determine how the right-hand side of (30) modifies the dispersion relation (23). We add, to a uniform counterflow $\mathbf{w}$, perturbations proportional to $\exp(\mathrm{i}\mathbf{k}\cdot\mathbf{x} - \mathrm{i}\omega t)$, and quickly find from (16) and (30) that (23) is replaced by

$$\omega^2 = c^2k^2(1 + \tfrac{1}{2}a^2k^2) + \mathrm{i}\zeta\rho_\infty k^2(\omega - \mathbf{w}\cdot\mathbf{k}). \tag{31}$$

For small ζ, the roots of (31) are approximately real; one of them is $\omega \approx \omega_r = ck(1 + \frac{1}{2}a^2k^2)^{1/2} > 0$, and its imaginary part is defined by the imaginary part of (31):

$$\omega_i \approx -(\zeta\rho_\infty k^3/2\omega_r)\left[w - c(1 + \tfrac{1}{2}a^2k^2)^{1/2}\right]. \tag{32}$$

If $w < c$, this is positive for all k, but if $w > c$ it is negative for all sufficiently small k, so establishing the breakdown of superfluidity once the Landau critical velocity (here c) is exceeded.

Although, as shown by Berloff (1999), the ζ term can be a useful practical tool in computing vortex structure, our interest in ζ in this review is that it represents a potentially significant source of non-thermal quasi-particles. Consider superflow past a body such as a positive ion. It is convenient, as in §6 below, to treat the body as an infinite potential barrier to the condensate, and if this is done the GP equation allows the superfluid to have *any* velocity along the boundary. In reality, however, ψ penetrates a very short distance into the body and collisions within the solid can generate quasi-particles that, on average, move with it. In the parlance of fluid mechanics, the normal fluid velocity $\mathbf{u}_n$ obeys the no-slip condition on the boundary $\mathbf{u}_n = 0$. The $\zeta-$term leads to quasi-particle emission whenever the superflow along the boundary exceeds the Landau critical velocity; for the local GP model, the quasi-particles are seen as sound waves (phonons).

It may be worth pointing out that the condition $w > u_L$ for the destruction of superfluidity is invalid where healing occurs and the $\nabla^2\rho^{1/2}$ term in (17) or (30) is significant. The superfluid vortex provides a prime example, in which $u_s \to \infty$ in the vortex core, although no instabilities are seen in numerical simulations (provided the vortex as a whole does not move with super-Landau speeds; see Berloff and Roberts (1999). For the remainder of this review, $\mathbf{u}_s$ will again be denoted by $\mathbf{u}$.

Finally, we should not ignore what is perhaps the most fundamental objection to GP theory. Although by including $\hbar$ it provides the verisimilitude of being a quantum description of superfluidity, it is in reality semi-classical. A proper operator description is, however, so complex that it cannot be usefully employed to study situations as complicated as those described in this review. We should not, however, overlook the progress that has been made towards a more realistic description of a vortex core (see [46]).

4 Vortices

A vortex line is defined by a zero of the wave function $\psi = 0$. The straight-line vortex creates a velocity around this line of $u = \hbar/Ms$, where s is the distance from the vortex line. The equation for the amplitude of the steady straight-line vortex is found by substituting $\psi = R(s)\exp(\mathrm{i}\chi)$ into (8) written in cylindrical coordinates (s, χ, z):

$$\frac{d^2R}{ds^2} + \frac{1}{s}\frac{dR}{ds} - \frac{1}{s^2}R + R - R^3 = 0, \tag{33}$$

where distance is scaled by a and R by R_∞. For small distances from the axis, R is proportional to s; for $s \to \infty$, $R \sim 1 - 1/2s^2$. The energy per unit length of the vortex line is

$$\mathcal{E}_\ell = \frac{\kappa^2\rho_\infty}{4\pi}\left(\int_0^\infty \left[\frac{dR}{ds}\right]^2 s\,ds + \int_0^\infty \frac{R^2}{s}\,ds + \frac{1}{2}\int_0^\infty (1-R^2)^2 s\,ds\right). \tag{34}$$

The first term can be regarded as a “quantum energy”, the second term is the classical vortex kinetic energy that diverges logarithmically unless a cut-off distance L is introduced; the third term in (34) represents the potential energy. The energy per unit length of the vortex is usually expressed in the form

$$\mathcal{E}_\ell = \frac{\rho\kappa^2}{4\pi}\left(\ln\frac{L}{a} + L_0\right), \tag{35}$$

where the constant L_0 is called the “vortex core parameter” and was determined numerically by Pitaevskii [40] as $L_0 = 0.3809$.

A dense array of straight-line vortices are encountered when a bucket of superfluid is rotated rapidly. This greatly affects its dynamics. This gives rise to HVBK theory; see, for example Hills and Roberts [29] and Holm (this meeting).

Straight-line vortices can transmit energy along their length by Kelvin waves. These have been comprehensively analyzed for incompressible Euler fluids; see for example Chapter 11 of Saffman [47]. They have been less well studied for compressible fluids such as the GP condensate, for which the Kelvin wave may be accompanied by acoustic emission that ultimately damps out the waves, unless they are sustained by a source.

This emission is of interest in studies of superfluid turbulence (§5). According to the analysis of Pitaevskii [40], the Kelvin waves that bend the rectilinear vortex do not emit sound if their wavelength is sufficiently long; more general types of wave have been studied by Rowlands [45].

Large vortex rings were investigated by Roberts and Grant [44] and they obtained the following expressions for the energy per unit length, momentum, and velocity, v:

$$\mathcal{E} = \tfrac{1}{2}\rho\kappa^2 R\left(\ln\frac{8R}{a} + L_0 - 2\right), \quad p = \rho\kappa\pi R^2, \tag{36}$$

$$v = (\kappa/4\pi R)\left(\frac{8R}{a} + L_0 - 1\right). \tag{37}$$

As expected, $\mathcal{E} \approx 2\pi R\mathcal{E}_\ell$, but also rings obey Hamilton's equation

$$v = \partial\mathcal{E}/\partial p. \tag{38}$$

Jones and Roberts [33] determined the entire sequence of vortex rings numerically for the GP model (8). They calculated the energy $\mathcal{E}$ and momentum p and showed how the location of the sequence in the $\mathcal{E}p$-plane relates to the superfluid helium dispersion curve. They found two branches meeting at a cusp where p and $\mathcal{E}$ assume their minimum values, p_m and $\mathcal{E}_m$. As $p \to \infty$ on each branch, $\mathcal{E} \to \infty$. On the lower branch the solutions are asymptotic to the large vortex rings (36)-(37). Since the GP model has a healing length (based on the sound velocity) different from the vortex core parameter there are two possible ways to introduce dimensional units and to plot the solitary wave sequence next to the Landau dispersion curve on the $p\mathcal{E}-$ plane. If the dimensional units based on the vortex core parameter are chosen, the cusp lies just above the Landau dispersion curve; if instead the healing length (sound speed) is selected the cusp meets the dispersion curve of the GP model, which (we recall) does not have a roton branch.

As $\mathcal{E}$ and p decrease from infinity along the lower branch, the solutions begin to lose their similarity to large vortex rings, and (36) - (37) determine $\mathcal{E}$, p, and v less and less accurately, although (38) still holds. Eventually, for a momentum p_0 slightly greater than p_m, the rings lose their vorticity (ψ loses its zero), and thereafter the solitary solutions may better be described as 'rarefaction waves'. The upper branch consists entirely of these and, as $p \to \infty$ on this branch, the solutions asymptotically approach the rational soliton solution of the Kadomtsev - Petviashvili (KP) equation and are unstable.

An interesting, and still incompletely answered question is whether the GP sequence of solitary waves is stable or not. The question is not frivolous since the classical circular rings in an incompressible fluid are known to be unstable (Widnall and Sullivan [54]). Jones *et al.* [32] concluded that the entire upper branch of rarefaction waves [33] is unstable, but that the lower branch solutions may be stable because their axisymmetric expansion or contraction is forbidden due to energy and momentum conservation. Grant [23] examined asymmetric perturbations of a large ring in the form of infinitesimal Kelvin waves, but he did not locate any that grew and, moreover, his analysis is inconclusive since it omitted the acoustic emission that accompanies the Kelvin waves. This was however included by Pismen and Nepomnyashchy [39], who found that it is stabilizing.

5 Superfluid turbulence; vortex line reconnection

Superfluid turbulence has been the focus of many experimental studies (e.g., [52], [18]), especially in "the high temperature regime," by which we mean $0.6°K \leq T < T_\lambda \approx 2.172°K$, where T_λ is the λ-point, which marks the transition between the normal and superfluid phases of helium. In this regime, the density, ρ_s, of superfluid is smaller than the normal fluid density, ρ_n, and in consequence turbulence in the superfluid is, to a large degree, determined by the turbulence taking place in the normal fluid. This is reflected by the success of theories of superfluid turbulence, such as that of Barenghi *et al.* [1], [2], in which the superfluid vorticity is largely tied to that of the normal fluid. In contrast, in the low temperature range ($T \leq 0.6°K$), where ρ_n is smaller than ρ_s, we may expect turbulence in the superfluid largely to determine turbulence in the normal fluid, rather than the reverse.

For the study of superfluid turbulence in the low temperature range it is necessary to follow the evolution of only two fields, the real and imaginary parts of ψ, rather than ρ and $\mathbf{v}$, or ρ and a non-single-valued velocity potential ϕ. There is however no high wavenumber sink of energy to terminate the Kolmogorov cascade. This obstacle may restrict the use of the simplest forms (1) or (8) of the GP model for turbulence studies, but the Carlson generalization, that uses (30 instead of (17), may be the remedy, since this recognizes that, in real helium even in the low temperature range, normal fluid is present that is coupled to the superfluid and which, through its viscosity, provides a high wavenumber sink. Another difficulty is that strong turbulence contains a complicated mixture of condensate, phonons, rotons, quantized vortices, vortex waves and shocks. Such a variety of processes may make it difficult to determine universal scaling laws for the turbulent correlation functions.

Recently several papers have appeared that discuss decaying Kolmogorov turbulence using GP theory. Nore *et al.* [38] studied superfluid turbulence using numerical simulations of the GP model. They decomposed the total energy (which is conserved) into incompressible kinetic, internal, and "quantum" components (that corresponds to acoustic excitations), and they computed the corresponding energy spectra. They found that the rate of transfer of kinetic energy into other energy components is comparable with the rate of energy dissipation through viscosity in classical turbulence. At the moment of maximum energy dissipation, the energy spectrum resembles the Kolmogorov inertial range.

The term "superfluid turbulence" is often used synonymously for the "evolution of a superfluid vortex tangle". The dynamics of the turbulent state depend crucially on the interactions of the vortex filaments. In a set of pioneering papers, Schwarz [48] developed a numerical technique to simulate the dynamics of the vortex tangle. This was based on the classical theory of vortex filaments in an incompressible Euler fluid. The reconnection of vortex lines was therefore forbidden by Kelvin's theorem, and he was therefore compelled, when studying changes in vortex line topology, to introduce *ad hoc* reconnection rules, e.g., that vortex filaments reconnect if, and only if, they approach within a distance of Δ of one another, where Δ is an *ad hoc* constant of the order of the core radius. As we saw in §2 above, Kelvin's theorem does not apply to GP models when a zero of ψ lies on the circuit Γ in (22). The coalescence of vortex lines merely corresponds to the merging of two zeros of ψ, and the creation of vortices corresponds to the appearance of a new zero line of ψ. These processes were first seen to happen in the GP calculations of Jones and Roberts [33] and later, in a more graphic form, by Koplik and Levine ([35] and [36]), who simulated the interaction between straight-line vortices and their reconnection. They also witnessed the annihilation of vortex rings of similar radii. Vortices can also be nucleated by moving bodies such as ions, but again this process cannot occur in an Euler fluid, but is allowed by the GP models, as is seen in the next Section. Another grave disadvantage of using the incompressible Euler

Fig. 1. The evolution of eight straight-line vortices in 2D within a box, four of each direction of circulation. As a result of the interactions, the number of vortices decreases and their energies are transmitted to sound waves

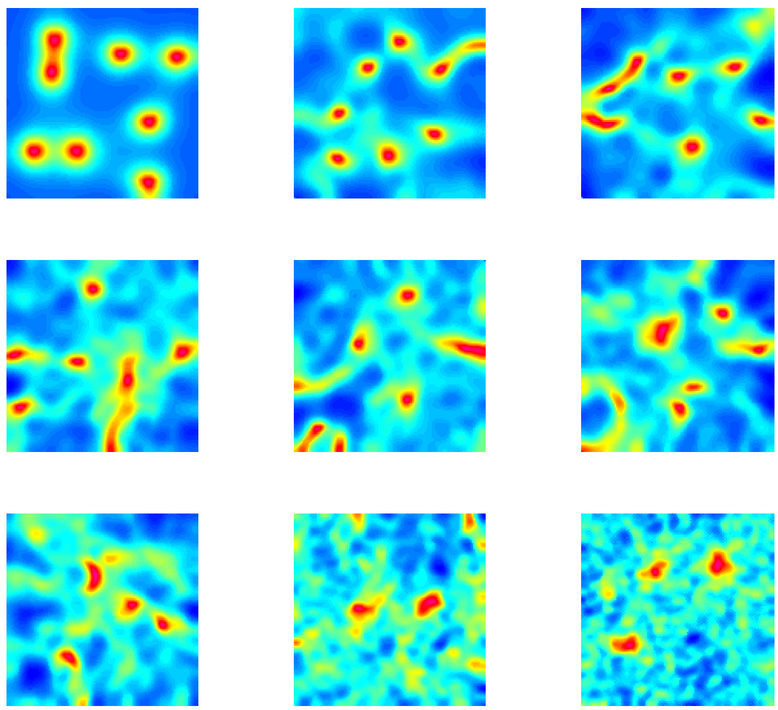

fluid to model the superfluid is that it eliminates sound in transferring, and perhaps cascading, energy down the turbulence spectrum. Vinen (this meeting) has stressed the potential importance of this process. Although the simplest form (8) of GP theory gives c incorrectly (see §1), the generalized theory to be described in §8 below, may provide a viable route to progress. Svistunov [51] has stressed the role of Kelvin waves in the turbulent cascade.

In Figure 1, the results of unpublished calculations by Berloff of the evolution of two-dimensional solutions of (8) are shown, in terms of the density ρ which, being depleted near a vortex core, is a clear marker for the line vortices. The walls of the computational box were taken to be reflective. It may be seen that the number of vortex lines is not conserved during the simulation; vortex nucleation and annihilation occurs. At the start there were 4 vortices of positive circulation and 4 of negative circulation. Over the period of integration the energy is increasingly transferred to sound waves and the number of vortices gradually diminishes.

6 Intrinsic vortex nucleation

In this section we consider the nucleation of quantized vortices from the standpoint of GP theory. Understanding vortex nucleation and the critical velocities associated with it is one of the most significant questions of superfluidity. Breakdown of ideal superflow in channels and in rotating containers is usually attributed to the formation of vortices. Flow through apertures and around impurities is known to generate vortex rings and vortex loops. According to Donnelly [18] we should distinguish between 'extrinsic nucleation', which concerns the growth of pre-existing vorticity from 'intrinsic nucleation', which is creation of vorticity from "nothing". It is virtually impossible to distinguish between these two experimentally. The energy of the trapped vortex may be close to the energy of an elementary excitation such as a roton. It could have been excited thermally and remained trapped at a pinning center during the cooling down of the superfluid to low temperatures, and then be enlarged and "released" by superflow past that center.

The intrinsic nucleation is hard to understand as there is no truly microscopic theory of the superfluid. We do not know how to describe the processes on the scale of the coherence length, where the motion is governed by the full quantum many-body structure of the superfluid. We confine attention here therefore to two possible approaches to vortex nucleation. The first is based on the GP model; the second relies on semiclassical, hydrodynamic (large-scale) theory with the vortex assumed *ab initio* with tunneling introduced in an *ad hoc* way. As was emphasized by Fischer [20], and foreshadowed long ago by, for example, Schwarz and Jang [50], there are difficulties faced by the quasi-classical theory of nucleation that render it incapable of describing intrinsic nucleation. A semiclassical description is valid only if the quantum core structure of the tunneling object does not come into contact with the boundary. The principal advantage of using the GP model is that semiclassical and tunneling processes are joined seamlessly.

Vortex nucleation by an impurity such as the positive ion ${}^4\mathrm{He}_2^+$ moving in superfluid helium at low temperature with velocity v has been studied experimentally and theoretically (see, e.g. Donnelly, 1991), and has uncovered some interesting physics. The flow round an ion that is moving with a sufficiently small velocity, v, is well represented by one of the classical solutions of fluid mechanics, namely the flow of an inviscid incompressible fluid around a sphere. In this solution, the maximum flow velocity, $\mathbf{u}$, relative to the sphere is $3v/2$, and occurs on the equator of the sphere (defined with respect to the direction of motion of the sphere as polar axis). Above some critical velocity, v_c, the ideal superflow around the ion breaks down, leading to the creation of a vortex ring (Rayfield and Reif, 1964). Muirhead *et al.* [37] created a theory of vortex nucleation that allowed them to estimate three useful quantities (i) v_c, (ii) the form of the potential barrier that must be overcome for the creation of vortices both as encircling rings and vortex loops, and (iii) the nucleation rate. These calculations were carried out for a smooth rigid sphere moving through an ideal incompressible fluid using the semiclassical approach.

An important scale defined by the condensate model is the 'healing length', a, defined in (19). This determines the radius of a vortex core and the thickness of the 'healing layer' that forms at a potential barrier (such as the ion surface in GP model). The radius, b, of the ion is large compared with a, and asymptotic solutions for $\epsilon \equiv a/b \to 0$ become relevant. Such a solution has two parts, an interior or 'boundary layer' structure that matches smoothly to an exterior or 'mainstream' flow. Berloff and Roberts [6] showed that the dimensionless flow velocity $\mathbf{U} = \mathbf{u}/c$ is greatest on the equator of the sphere where it is

$$U_\theta = 3V/2 + 0.313V^3 + 0.3924V^5 + 0.648V^7 + 1.24V^9 + 2.63V^{11} + \cdots \quad (39)$$
$$+\epsilon\Big(2.12V + 1.58V^3 + 2.89V^5 + \cdots\Big),$$

where $V = v/c$. This gives $v_c \approx 0.53c$ for $\epsilon \to 0$. (We recall here that the criterion $u = c$ for criticality strictly applies only for $\epsilon = 0$; see §3.)

There is some similarity between the flow of the condensate past the ion and the motion of a viscous fluid past a sphere at large Reynolds numbers, the healing layer being the counterpart of the viscous boundary layer. There are, however, important differences. At subcritical velocities, the flow of the condensate is symmetric fore and aft of the direction of motion, and the sphere experiences no drag. In contrast, the viscous boundary layer separates from the sphere, so evading D'Alembert's paradox, destroying the fore and aft symmetry, and therefore bringing about a drag on the sphere. Moreover, when $v > v_c$, shocks form at or near the sphere, but shocks are disallowed in the condensate since they represent a violation of the Landau criterion and a breakdown of superfluidity. When $v > v_c$, the condensate evades shocks through a different mode of boundary layer separation. The sphere sheds circular vortex rings that move more slowly than the sphere and form a vortex street that trails behind it, maintained by vortices that the sphere sheds. As the velocity of the ion increases such a shedding becomes more and more irregular. Each ring is born at one particular latitude within the healing layer on the sphere. As it breaks away into the mainstream, it at first contributes a flow that depresses the mainstream velocity on the sphere below critical. As it moves further downstream however, its influence on the surface flow diminishes. The surface flow increases until it again reaches criticality, when a new ring is nucleated and the whole sequence is repeated. The vortex street trailing behind the ion creates a drag on the ion that decreases as the nearest vortex moves downstream, but which is refreshed when a new vortex is born.

Berloff [4] considered the vortex nucleation when the symmetry of the system is broken in the presence of the random noise or by introducing a plane wall at some distance from the ion. Figure 2 shows the formation and evolution of a vortex loop on the positive ion when it moves subcritically. As the velocity reaches criticality on the side of the sphere closer to the boundary, a vortex loop appears, spreads laterally, interacts with the boundary, the feet of the vortex line on the surface of the ion come closer to one another, and they detach to form a loop on the boundary.

Fig. 2. The results of numerical integration of (3) for the positive ion moving with the velocity $0.51c$ for the isosurface $\varrho = 0.2\varrho_\infty$ at (a) $t = 132a/c$, (b) $t = 168a/c$, (c) $t = 216a/c$, and (d) $t = 240a/c$.(After [4])

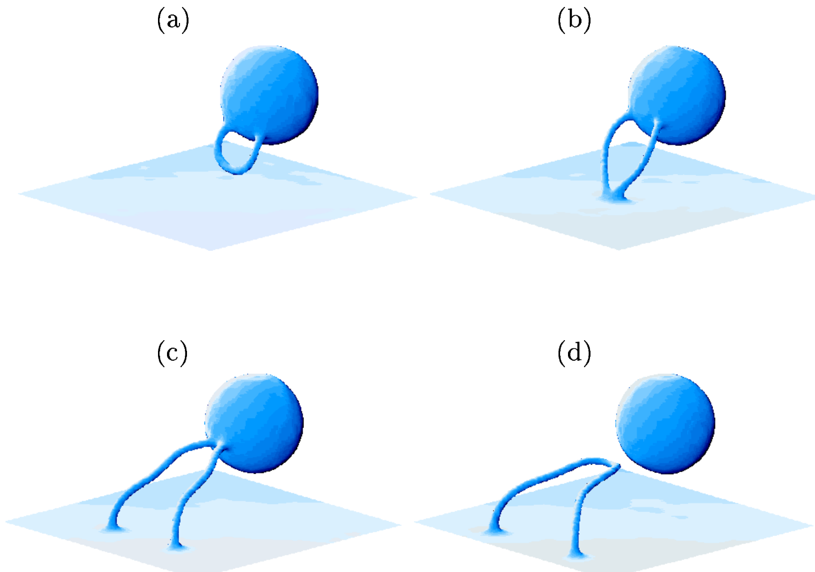

Frisch *et al.* [21] and Winiecki *et al.* [55] have solved numerically the condensate equation for flow past a circular cylinder and Berloff and Roberts [6] for the flow around a positive ion and have confirmed the main features of the scenario just described. Below the critical velocity steady solutions of the GP model exist. Huepe and Brachet [31] numerically computed stationary steady and unsteady solutions for flow around a cylinder. They confirmed the critical velocity of nucleation $v_c \approx 0.42c$ found numerically by Frisch *et al.* [21] and Winiecki *et al.* [55] and through the asymptotic expansion by Berloff and Roberts [6]. Winiecki *et al.* [56] carried out integrations similar to those of Huepe and Brachet [31] but for three dimensional flow around a penetrable sphere. They also found three branches of steady solutions that exist up to the nucleation point. In order of decreasing energy these are (i) irrotational flow round the sphere, (ii) a vortex loop attached to the sphere, and (iii) a vortex ring surrounding the sphere symmetrically. These three solutions are all stable. Perhaps a transition from one branch to another can be achieved by quantum tunneling in the way envisaged by Muirhead *et al.* [37].

In addition to the positive ion, other impurities have proved to be useful experimental probes, including neutral atoms such as ^{3}He (radius $\sim$ 4Å) and the negative ion, which is an electron in a bubble cut out of the liquid owing to the repulsive interaction between the electron and surrounding helium atoms. We now consider the negative ion.

In the Hartree approximation, the equations governing the one particle wavefunction of the condensate, ψ, and the wave function of the electron, ϕ, are a pair of coupled equations suggested by Gross [27] and by Clark [14], [15]:

$$\mathrm{i}\hbar\frac{\partial\psi}{\partial t} = -\frac{\hbar^2}{2M}\nabla^2\psi + (U_0|\phi|^2 + V_0|\psi|^2 - E)\psi, \tag{40}$$

$$\mathrm{i}\hbar\frac{\partial\phi}{\partial t} = -\frac{\hbar^2}{2\mu}\nabla^2\phi + (U_0|\psi|^2 - E_e)\phi, \tag{41}$$

where M and E are the mass and single particle energy for the bosons; μ and E_e are the mass and energy of the electron. The interaction potentials between boson and electron and between bosons are here assumed to be of $\delta-$function form $U_0\delta(\mathbf{x} - \mathbf{x}')$ and $V_0\delta(\mathbf{x} - \mathbf{x}')$, respectively. To lowest order, perturbation theory predicts such interaction potentials to be $U_0 = 2\pi l\hbar^2/\mu$ and $V_0 = 4\pi d\hbar^2/M$, where l is the boson-impurity scattering length, and d is the boson diameter. The normalization conditions on the wave functions are

$$\int |\psi|^2 dV = N, \qquad \int |\phi|^2 dV = 1. \tag{42}$$

Using the system (40)-(41), Grant and Roberts [25] studied the motion of a negative ion moving with speed v using an asymptotic expansion in v/c, where c is the speed of sound, so that their leading order flow is incompressible. Treating $\epsilon \equiv (a\mu/lM)^{1/5}$ as a small parameter they calculated the effective (hydrodynamic) radius and effective mass of the electron bubble. By employing a convergent series expansion suitable for $\mathbf{u}$ = $\mathcal{O}(c)$, Berloff and Roberts (2000) determined v_c in the limit $\epsilon \to 0$. They have shown that v_c for the negative ion is about 20% less than v_c for the positive ion, in agreement with the experimental findings of Zoll (1976); see also Table 8.2 of Donnelly (1991). This reduction may be attributed to the flattening of the electron bubble by its motion through the condensate. The "equatorial bulge" is created by the difference in pressure between the poles and equator associated with the greater condensate velocity at the latter than at the former. The existence of the bulge also enhances these differences in velocity (and pressure), as compared with a spherical impurity, with the result that, if v is gradually increased from zero, the flow u_e on the equator of the electron bubble attains the velocity of sound before u_e does for the positive ion.

Finally, we mention the nucleation of the vorticity by superfluid flow through apertures. Burkhart *et al.* [11] considered the properties of a vortex close to a wall as derived from the GP model and obtained a critical velocity and vortex radius at nucleation that agree with experiments.

7 Capture of impurities by vortex lines

Rayfield and Reif [43] used an ion time-of-flight spectrometer to determine the dynamics of ion-quantized vortex ring complexes. They observed that above some critical velocity, v_c, ideal superflow around an ion breaks down. The moving ion produces vortex rings and the ion becomes trapped in one of these. The capture of negative ions by quantized vortex lines in a rotating bucket was first demonstrated by Careri *et al.* [12]. Schwarz and Donnelly [49] observed that at low temperatures (< 0.5 K) straight-line vortices can trap positive ions.

Berloff and Roberts [8] solved equations (40)-(41) numerically to observe and elucidate the process of capture; see Figure 3. They have shown that this process can be better characterized as the reconnection of the vortex line with its pseudo-image inside the impurity. Initially the vortex line bends towards the impurity at the point where the distance between them is least. As the result of this interaction the impurity moves around the vortex axis. The process of capture continues as the vortex line terminates on the surface of impurity and its feet move to opposite poles of the impurity surface. At the same time helical waves start propagating from the impurity along the two segments of the vortex line. Such helical waves have been observed during the relaxation of the vortex angle when two vortex lines reconnect [28], and are just Kelvin waves. These waves, and associated sound waves, radiate energy to infinity.

During the time in which the vortex merges with the healing layer round the ion (now the layer of thickness $\sim a$ in which neither ϕ in (40) nor ψ in (41) can be neglected), the character of the solution alters rapidly, corresponding to the topological change that defines the capture of the ion by the vortex. Once the vortex has divided into two, with separate feet attached to the healing layer, the flow round the ion has acquired circulation that it previously could not possess.

It is clear from the discussion above that the trapped impurity is in the lower energy state than the free impurity. The difference $\triangle V$ is the 'substitution energy', also called the 'binding energy'. Donnelly and Roberts [17], using the healing model of the vortex core, estimated that

$$\triangle V = 2\pi\rho_s(\hbar/M)^2 b\left[(1+a^2/b^2)^{1/2}\sinh^{-1}(b/a)-1\right]. \tag{43}$$

The more sophisticated calculations of Berloff and Roberts [8] gave 21.7 K for a positive ion of radius $10a$, where $a = 0.47$ Å for the nondimensionalization based on the speed of sound. If instead $a = 1$ Å is used, they obtained $\triangle V/k_B \approx 46$ K, which may be compared with 33.5 K according to (43). For the electron bubble our result is $\triangle V/k_B = 55$ K, and (43) gives $\triangle V/k_B = 66$ K if $R = 16$ Å is used. The healing layers around the positive and negative ions differ dramatically and the healing layer close to the vortex feet is less depleted, which was not taken into account by (43). This explains why (43) overestimates $\triangle V$.

The capture of a penetrable sphere moving with supercritical velocity by a vortex ring that it itself created was simulated by Winiecki and Adams [57] through the full 3D numerical integration of the GP equation, supplemented with the calculation of the drag on the surface of the sphere. They have shown that after the positive ion emits the vortex ring, the drag on the ion slows it down and the ion is captured by the vortex ring; see Figure 4.

Berloff and Roberts [7] performed integrations of (40)-(41) for the following configuration: a moving negative ion catches up with a vortex ring moving in the same direction. The axis of the ring does not coincide with the axis of the impurity. Such a condition is necessary to destroy the axisymmetry of the system. Figure 5 shows the process of capture of the electron by the vortex ring. Initially, the faster moving ion

Fig. 3. The results of numerical integration of (40)-(41) for the negative ion initially placed a distance $6a$ apart from the rectilinear vortex line. The pictures show the isosurface $\varrho = 0.2\varrho_\infty$. (After [8])

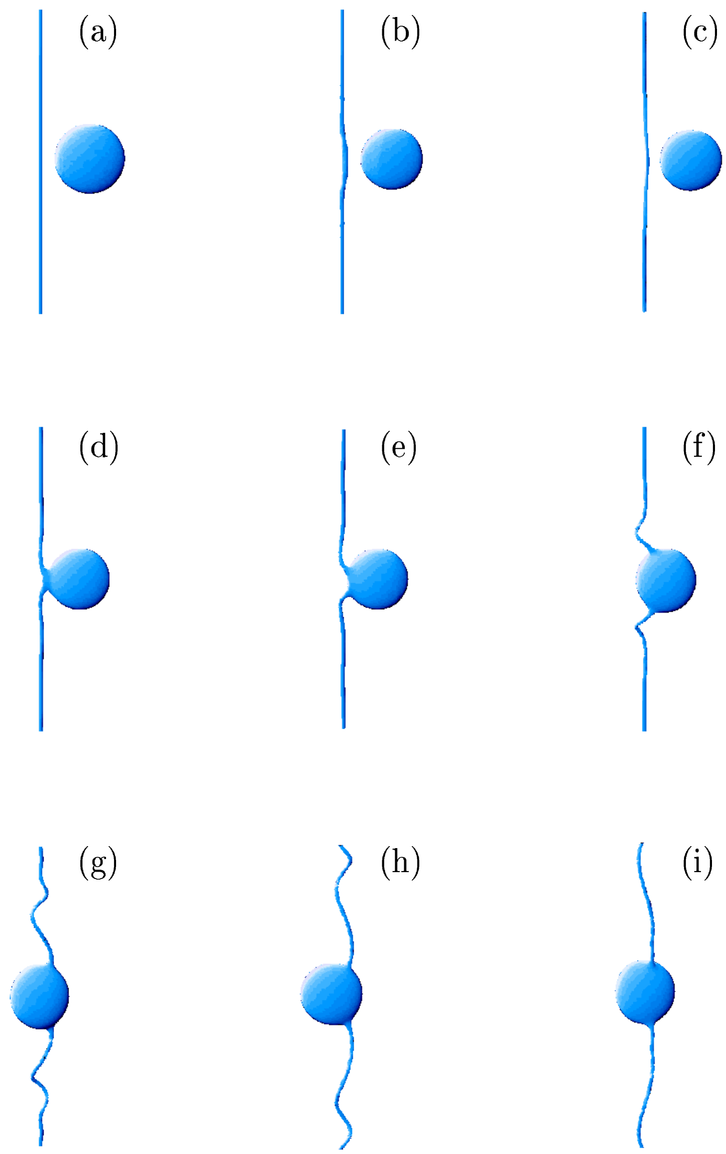

Fig. 4. Capture of the penetrable sphere by the vortex it itself created for different values of the applied force. (After [57])

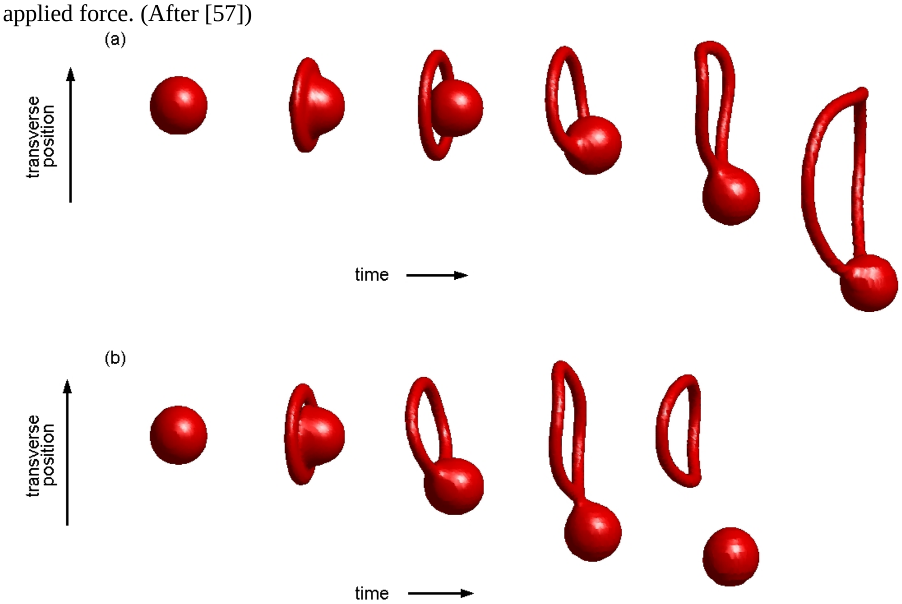

passes the vortex ring. The Bernoulli effect of the flow propels the ion and vortex towards one another with a force approximately proportional to s^{-3}, where s is the closest distance between them, similarly to the process of capture of the ion by a straight line vortex.

Fig. 5. Capture of the moving ion by the vortex ring: the results of numerical integration of (40)-(41) for the isosurface $\varrho = 0.2\varrho_\infty$. (After [7])

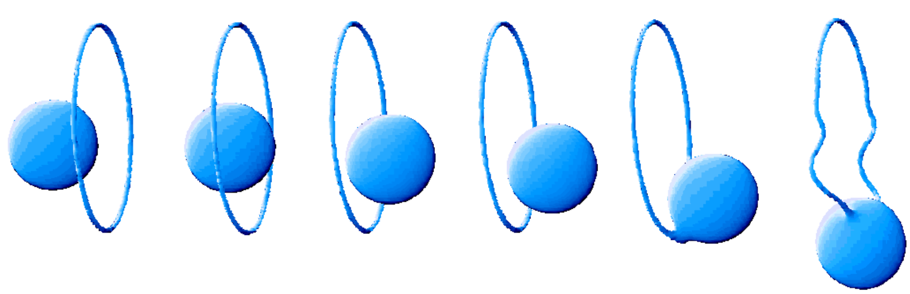

8 Nonlocal models

In §3 we considered different shortcomings of the GP model. The natural question arises whether it is possible to remedy (3) to make it more quantitatively realistic for superfluid helium. For some time there has been a belief that, as soon as the nonlocal model (1) with a realistic two-particle potential, V, that leads to phonon-roton-like spectra is solved, the properties of superfluid helium will be well represented. The minimum requirements on such a potential would be (i) the correct position of the roton minimum and (ii) the correct speed of sound. Actually such a fit can be obtained with a variety of potentials. Pomeau and Rica [41] pioneered the use of nonlocal models for study superfluidity, but their model did not have the correct sound velocity (slope of the dispersion curve at the origin). Berloff [3] investigated the applicability of (1) with a potential that adequately represents the dispersion curve. It was shown that for liquid helium having the correct Landau dispersion curve, solutions of equation (1) develop non-physical mass concentrations. In particular, the “Eulerian part” of the momentum equation (without the quantum stress tensor) may become no longer hyperbolic in some parts of the integration volume. A virial theorem, similar to the one used to establish the catastrophic blow-up in the focusing nonlinear Schrödinger equation, can be used to establish similar catastrophes in bounded volume for (1). This indicates that the assumptions underlying the derivation of the equation break down and that higher order nonlinearities must be introduced.

A more accurate approach in modeling liquid helium is through density-functional theory done by Dalfovo *et al.* [16], which attempts to give an adequate microscopic description of interactions. In this approach the total energy is still written as a functional of the one-body density, but it includes short-range correlations [19]. This approach has provided a quantitatively and qualitatively reliable representation of the superfluid properties of free surfaces, helium films, and droplets (see [16] and references therein). At the same time this approach is phenomenological and results in rather complicated forms of the energy functionals with many parameters that are chosen to reproduce liquid helium properties.

Berloff and Roberts [5] attempted to modify the nonlocal model (1) in the spirit of a density - functional approach, by introducing only one additional nonlinear term in the expression for the correlation energy. This allowed them to remedy the nonphysical features of model (1), while retaining not only an adequate representation of the Landau dispersion relation, but also simplicity in the analytical and numerical studies.

The correlation energy of the Skyrme interactions in nuclei [53] is given by

$$W_c(\rho) = \frac{1}{M^2}\int\left[\frac{W_0}{2}\rho^2 + \frac{W_1}{2+\gamma}\rho^{2+\gamma} + W_2(\nabla\rho)^2\right], \tag{44}$$

where W_0, W_1, W_2 and γ are phenomenological constants. The first two terms give a local density approximation, and the gradient term corresponds to finite range interactions. The necessary nonlocality of interactions was added directly into the first term of (44) by introducing a two-body interaction potential, $V(|\mathbf{x}-\mathbf{x}'|)$, so that (44) becomes

$$W_c(\rho) = \frac{1}{M^2}\int\left[\frac{1}{2}\int \rho(\mathbf{x})V(|\mathbf{x}-\mathbf{x}'|)\rho(\mathbf{x}')\,d\mathbf{x}' + \frac{W_1}{2+\gamma}\rho^{2+\gamma}\right]\,d\mathbf{x}. \tag{45}$$

This incorporates and generalizes the W_2 interaction term in (44), which has therefore been abandoned; $V(|\mathbf{x}-\mathbf{x}'|)$ is chosen so that the implied dispersion relation is a good fit to the Landau dispersion curve. Following private communications with C. Jones, Berloff and Roberts [5] considered a potential of the form

$$V(|\mathbf{x}-\mathbf{x}'|) = V(r) = (\alpha + \beta A^2 r^2 + \delta A^4 r^4)\exp(-A^2 r^2), \tag{46}$$

and also the slightly modified potential

$$V(|\mathbf{x}-\mathbf{x}'|) = V(r) = (\alpha + \beta A^2 r^2 + \delta A^4 r^4)\exp(-A^2 r^2) + \eta\exp(-B^2 r^2), \tag{47}$$

where $A, B, \alpha, \beta, \delta$ and η are parameters that can be chosen to give excellent agreement with the experimentally determined dispersion curve.

On adopting (45), one can see that (1) is replaced by

$$i\hbar\Psi_t = -\frac{\hbar^2}{2M}\nabla^2\Psi + \Psi\int|\Psi(\mathbf{x}',t)|^2 V(|\mathbf{x}-\mathbf{x}'|)\,d\mathbf{x}' + W_1\Psi|\Psi|^{2(1+\gamma)}. \tag{48}$$

with (7) this equation becomes

$$i\hbar\psi_t = -\frac{\hbar^2}{2M}\nabla^2\psi + \psi\left(\int|\psi(\mathbf{x}',t)|^2 V(|\mathbf{x}-\mathbf{x}'|)\,d\mathbf{x}' + W_1|\psi|^{2(1+\gamma)} - E_v\right). \tag{49}$$

This model not only produces the structure and energy per unit length of the straight-line vortex that are very close to the ones obtained from the Monte Carlo simulations by Sadd *et al.* [46], but it also made it possible to bring the vortex core parameter (35) and the healing length into agreement. Figure 6 compares the experimentally determined dispersion curve with that employed by (49). The insets give the density in the core of the straight line vortex and in the healing layer at a solid boundary, both for (49) and for the GP model. The vortex rings of large radii satisfy (36)-(38). Berloff and Roberts [5] integrated (48) numerically to elucidate the behavior of the small vortex ring. The Berloff-Roberts calculations indicate that when the velocity of the vortex ring reaches the Landau critical velocity the ring becomes unstable and evanesces into sound waves. For any ring traveling with speed greater than the Landau critical velocity, the amplitude of the far-field solution will not decay exponentially at infinity, which makes the existence of such a ring impossible. One of the goals of these calculations was to clarify Onsager's concept of the roton as "the ghost of a vanished vortex ring." One can hope that the transition from the vortex ring to the sound pulse and the concomitant loss of vorticity would occur close to the roton minimum in energy-momentum space, or (more probable) close to the point where the group velocity and the phase velocity are equal (the Landau critical velocity u_L). Their calculations show that indeed there is a point on the $p\mathcal{E}-$ plane where the ring ceases to exist and where $u_L = \partial\mathcal{E}/\partial p$, but this point lies far from the roton minimum. It remains to be seen whether the idea of the roton as a ghostly vortex ring will ever be vindicated. As one has a great variety of potentials that lead to the Landau dispersion curve one can tune the parameters so that the line $\mathcal{E} = u_L p$, meets the $p\mathcal{E}-$ curve for the family of the vortex rings, to allow this sequence of vortex rings to be terminated at a lower energy and momentum level. Whether this process will lead to coalescence with the roton minimum is not yet clear.

Berloff and Roberts [9] used (49) to elucidate the differences between the processes of vortex nucleation and roton emission. They argued that vortices are nucleated when the velocity around the positive ion exceeds the velocity of sound. The moving ion generates rotons when it moves with the velocity greater than the Landau critical velocity.

Fig. 6. The dispersion relation $p - \mathcal{E}$. The solid line corresponds to the nonlocal potential $V(|\mathbf{x} - \mathbf{x}'|)$ with $A = 0.9$, $\chi = 0.2$, and $\gamma = 1$. The dots are based on experiment. The insets show (a) the amplitude $|\psi|/\psi_\infty$ of the straight line vortex for the nonlocal model (49) (solid line) and the GP model (dashed line); (b) the amplitude $|\psi|/\psi_\infty$ of the healing layer at a solid boundary (an infinite potential barrier) placed at $r = 0$ for the nonlocal model (solid line) and the GP model (dashed line); (c) the potential $V(|\mathbf{x} - \mathbf{x}'|)$ plotted as a function of $r = |\mathbf{x} - \mathbf{x}'|$, in the nondimensional units defined in [9]. (After [9])

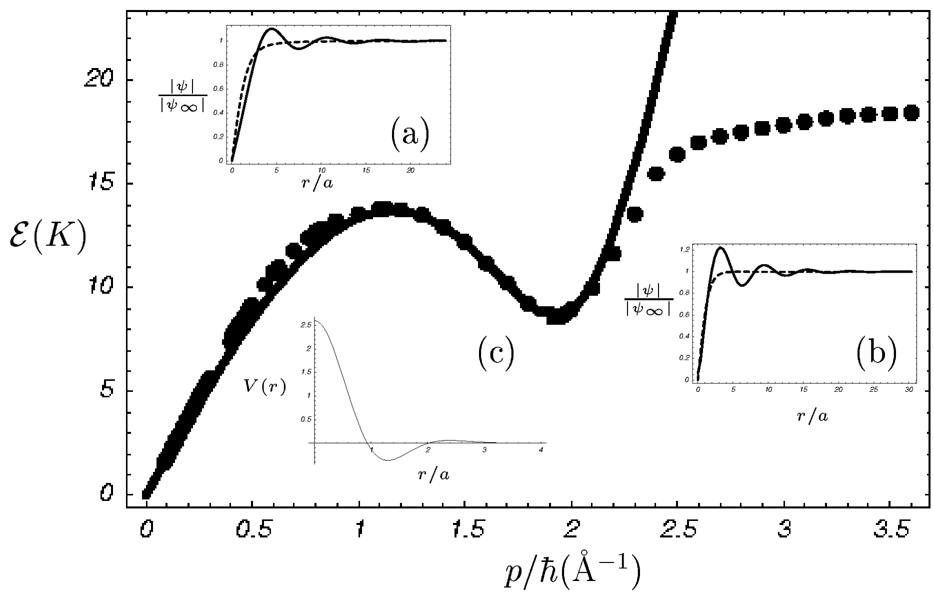

9 Conclusions

Despite the fact that the interatomic spacing in helium is short compared with the coherence length, the GP equation has proved itself useful in modeling, in at least a qualitatively faithful way, many of the phenomena that have been studied experimentally. This is partially a result of the great strides taken by computer technology during the past decade that have made it possible to undertake three-dimensional simulations of processes such as vortex-vortex and vortex-ion interactions, including the nucleation of vortices by ions and the capture of ions by vortices. It has also become possible to explore more general equations of Gross-Pitaevskii type from which a more realistic dispersion curve emerges, one that possesses a roton minimum at approximately the correct momentum and energy.

One topic that has not been addressed in this review concerns generalization to finite temperature. As is well known, the Landau two-fluid description of helium dynamics was devised before it was demonstrated that vorticity in the superfluid is quantized, and Landau theory encounters difficulties when quantized vortices are present . These difficulties are analogous to those encountered when the classical Euler equations are used to model the superfluid. One attempt to modify Landau theory in order to evade these difficulties was made by Hills and Roberts [30]. This theory was also, in a sense, a consequence of the one-fluid theory of Putterman and Roberts [42].

Despite the successes of Gross-Pitaevskii theory and its generalizations, much remains to be done, possibly by generalizing the theory itself, before it can realistically be used for superfluid helium. It is fortunate however that it can be legitimately applied to low density condensates, where the interatomic spacing is greater than the coherence length.

This review was written by two people whose backgrounds are in fluid mechanics. Not surprisingly therefore the perspective throughout has been fluid mechanical. Undoubtedly, we have neglected to cite work that we should have referenced. We apologize for any such omissions, which arise through ignorance and not malice.

Acknowledgments

We are grateful to "Sandy" Fetter for his criticisms of the previous version of this review, and "Lev" Pitaevskii and "Joe" Vinen for their helpful comments. This work is supported by the grant DMS-9803480 from the National Science Foundation.

References

1. C.F.Barenghi, D.C. Samuels, G.H. Bauer, R.J. Donnelly: Physics of Fluids **9**, 2631 (1997)
2. C.F.Barenghi, C.J. Swanson, R.J. Donnelly: J. Low. Temp. Phys.**100**, 385 (1995)
3. N.G. Berloff: J. Low. Temp. Phys. **116**, 359 (1999)
4. N.G. Berloff: Phys. Rev. Lett., submitted (2000)
5. N.G. Berloff, P. H. Roberts: J. Phys.: Math. Gen. **32**, 5611 (1999)
6. N.G. Berloff, P. H. Roberts: J. Phys.: Math. Gen. **33**, 4025 (2000)
7. N.G. Berloff, P. H. Roberts: J. Phys.: Math. Gen. accepted (2000)
8. N.G. Berloff, P. H. Roberts: Phys. Rev. B., accepted (2000)
9. N.G. Berloff, P. H. Roberts: Phys. Lett. A, in press (2000)
10. J. B. Brooks, R. J. Donnelly: J. Phys. Chem. Ref. Data **6**, 51 (1977)
11. S. Burkhart, M. Bernard, O. Avenel, E. Varoquaux: Phys. Rev. Lett. **72**, 380 (1994)
12. G. Careri, W. D. McCormick, F. Scaramuzzi: Phys. Lett. **1**, 61 (1962)
13. N.N. Carlson: Physica D **98**,183 (1996)
14. R.C. Clark: Phys. Lett. **16**, 42 (1965)
15. R.C. Clark: in *Superfluid Helium* ed. J. F. Allen (Amsterdam, North Holland, 1966)
16. F. Dalfovo, A. Lastri, L. Pricaupenko, S Stringari, J Treiner: Phys. Rev. B **52**, 1193 (1995)
17. R. J. Donnelly, P.H. Roberts: Proc. Roy. Soc.**A312**, 519 (1969)
18. R.J. Donnelly: *Quantized Vortices in Helium II*, (Cambridge University Press, Cambridge, 1991)

19. J. Dupont-Roc, M. Himbert, N. Pavlov, and J. Treiner: J. Low Temp. Phys. **81**, 31 (1990)
20. U.R. Fischer: Physica B **255**, 41 (1998)
21. T. Frisch, Y. Pomeau, S. Rica: Phys. Rev. Letts. **69**, 1644 (1992)
22. V.L. Ginzburg, L.P. Pitaevskii: Zh. Eksp.Teor. Fiz. **34**, 1240 (1958)
23. J. Grant: J. Phys. A: Gen. Phys. **4**, 695 (1971)
24. J. Grant: J. Phys. A: Math., Nucl. Gen. **6**, L151 (1973)
25. J. Grant, P. H. Roberts: J. Phys. A: Math., Nucl. Gen. **7**, 260 (1974)
26. E. P. Gross: J. Math. Phys. **4**, 195 (1963)
27. E. P. Gross: in *Quantum Fluids*. ed. D. B. Brewer (Amsterdam, North Holland, 1966)
28. F.R. Hama: Phys. Fluids **5**, 1156 (1962)
29. R.N. Hills, P.H.Roberts: Archiv. Rat. Mech. Anal. **66**, 43 (1977)
30. R.N. Hills, P.H.Roberts: J. Low Temp. Phys. **40**, 117 (1980)
31. C. Huepe, M. Brachet: C. R. Acad. Sci. Paris **325**, 195 (1997)
32. C.A. Jones, S. J. Putterman, P.H. Roberts: J. Phys. A: Gen. Phys. **19**, 2991 (1986)
33. C.A. Jones, P.H. Roberts: J. Phys. A: Gen. Phys. **15**, 2599 (1982)
34. I.M. Khalatnikov: *Introduction to the Theory of Superfluidity*, (W.A. Benjamin, Inc., New York Amsterdam, 1965)
35. J. Koplik, H. Levine: *Phys. Rev. Letts.* **71**, 1375 (1993)
36. J. Koplik, H. Levine: Phys. Rev. Letts. **76**, 4745 (1996)
37. C.M. Muirhead, W.F. Vinen, R.J. Donnelly: Phyl. Thans. R. Soc. Lond. A **3**, 433 (1984)
38. C. Nore, M. Abid, M. E. Brachet: Phys. Fluids **9**, 2644 (1997)
39. L.M. Pismen, A.A. Nepomnyashchy: Physica D **69**, 163 (1993)
40. L.P.Pitaevskii: Sov. Phys. JETP **13**, 451 (1961)
41. Y. Pomeau, S. Rica: Phys. Rev. Lett. **71**, 247 (1993)
42. S. J. Putterman, P. H. Roberts: Physica **117** A, 369 (1983)
43. G. W. Rayfield, F. Reif: Phys. Rev. **136**, A1194 (1964)
44. P.H. Roberts, J. Grant: J. Phys. A: Gen. Phys. **4**, 55 (1971)
45. G. Rowlands: J. Phys. A: Nucl. Gen. **6**, 322 (1973)
46. M. Sadd, G.V. Chester, L. Reatto: Phys. Rev. Lett. **79**, 2490 (1997)
47. P.G. Saffman: *Vortex Dynamics*, (Cambridge University Press, Cambridge, 1992)
48. K.W. Schwarz: Phys. Rev. B **38**, 2398 (1988)
49. K.W. Schwarz, R. J. Donnelly: Phys. Rev. Lett. **17**, 1088 (1966)
50. K.W. Schwarz, F. Jang: Phys. Rev. A **8**, 3199 (1973)
51. B. V. Svistunov: Phys. Rev. B **52**, 3647 (1995)
52. J. T. Tough: “Superfluid turbulence”. In *Progress in Low Temperature Physics*, **VIII**, ed. D.F. Brewer. Amsterdam: North-Holland, 133 (1982).
53. D. Vautherin, D. M. Brink: Phys. Rev. C **5**, 626 (1972)
54. S.E. Widnall, J. Sullivan: Proc. R. Soc. Lond. A **287**, 273 (1973)
55. T. Winiecki, J. F. McCann, C. S. Adams: Phys. Rev. Letts **82**, 5186 (1999)
56. T. Winiecki, J. F. McCann, C. S. Adams: Europhys. Letts **48**, 475 (1999)
57. T. Winiecki, C. S. Adams: Europhys. Letts submitted (2000)